This article is published as part of the *Dalton Transactions* themed issue entitled:

Dalton Transactions 40th Anniversary

Guest Editor Professor Chris Orvig, Editorial Board Chair
University of British Columbia, Canada

Published in issue 40, 2011 of *Dalton Transactions*

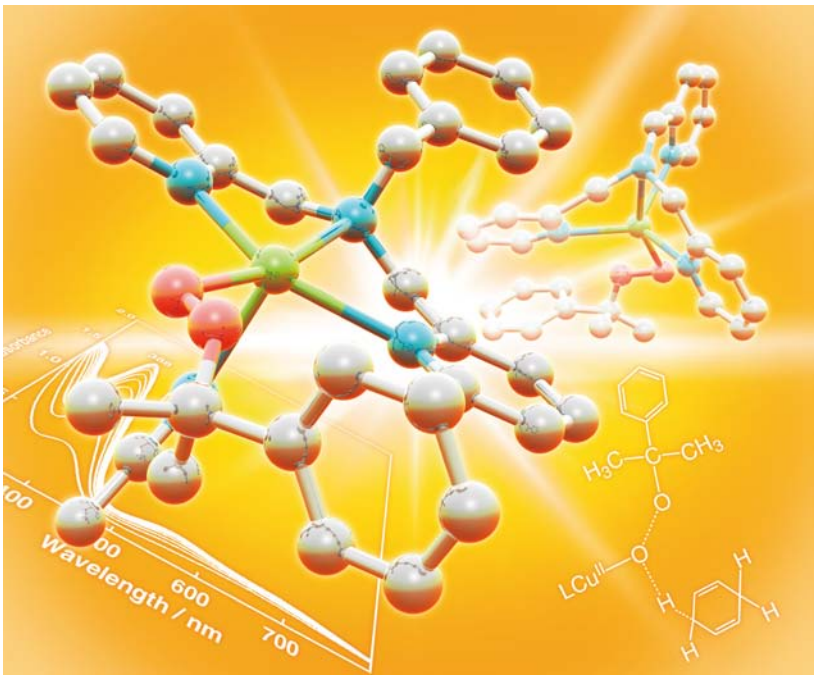

Image reproduced with permission of Shinobu Itoh

Welcome to issue 40 of the 40th volume of Dalton Transactions-40/40! Articles in the issue include:

PERSPECTIVE:

FRONTIER:

ARTICLES:

Visit the *Dalton Transactions* website for more cutting-edge inorganic and organometallic research
www.rsc.org/dalton

Dalton Transactions

Dynamic Article Links

Cite this: *Dalton Trans.*, 2011, **40**, 10535

www.rsc.org/dalton

PAPER

Cyclopalladated complexes of 4-aryl-2,1,3-benzothiadiazoles: new emitters in solution at room temperature†

Fabiana S. Mancilha,[a,b] Laurent Barloy,*[a] Fabiano S. Rodembusch,*[c] Jairton Dupont[b] and Michel Pfeffer[a]

Received 14th April 2011, Accepted 18th July 2011
DOI: 10.1039/c1dt10666j

The cyclopalladation of the 4-aryl-2,1,3-benzothiadiazoles **1a–c** with palladium acetate in acetic acid afforded the novel dimeric complexes **2a–c** in good yields. These were then converted into the monomeric pyridine-, chloro-coordinated cyclometallated complexes **3a–c** through reaction with lithium chloride in acetone and then pyridine in dichloromethane. All complexes were fully characterized by means of NMR, IR and elemental analysis. The X-ray structure of complex **2c** revealed that it presents transoid geometry, whereas the X-ray structure of **3c** shows that the pyridine ligand and the thiazole ring are mutually *trans*. Photophysical properties were investigated by means of UV-Vis absorption and fluorescence emission in solution. Solid-state diffuse reflectance UV-Vis spectra (DRUV) were also applied in order to better characterize the complexes photophysics in the solid state. All complexes present intense absorption at around 300 nm (λ_1) *via* ^{1}LC transitions located in BTD ligands, and additional low energy absorption bands, higher than 450 nm (λ_2) of ^{1}MLCT character. The complexes are fluorescent in solution at room temperature, where two emission bands could be observed, a high energy band (excitation @ λ_1) ascribed to the ligand emission and an additional red shifted low intense band (excitation @ λ_2) due to the complex emission.

Introduction

Fluorescent molecules have found widespread use in scientific and technological areas, especially as organic light-emitting diodes (OLEDs).[1–3] Although 2,1,3-benzothiadiazole (BTD) systems are among the most important nuclei in the chemistry of such luminescent compounds, studies concerning their synthesis and photoluminescent properties are relatively limited.[4–8] Indeed, most of these studies have been centred on the preparation and investigation of the photophysical properties of 4,7-disubstituted-2,1,3-benzothiadiazole derivatives. Moreover, examples in the literature of 2,1,3-thiadiazole derivatives as ligands of palladium(II) are rather rare.[9–15] Besides, the syntheses, characteristics and applications of cyclopalladated compounds have been extensively reviewed;[16–22] among them, five- and six-membered pallacyclic species are common. Therefore, it was reasonable to assume that 4-aryl-2,1,3-benzothiadiazoles could be cyclometallated and hence generate a new series of photoluminescent organometallic compounds in relation to well-known fluorescent cyclopalladated reported in the literature (Scheme 1).[23–26] We report hereafter that these dyes can generate a new family of cyclopalladated derivatives, the photophysical properties of which have been investigated.

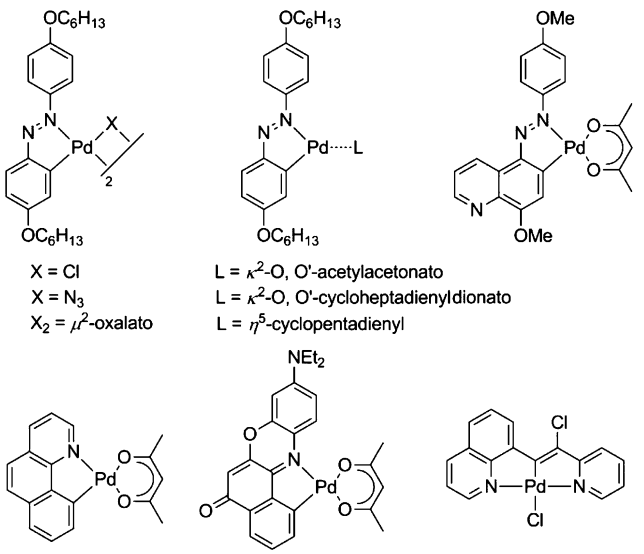

Scheme 1 Fluorescent cyclopalladated complexes reported in the literature.

[a]*Institut de Chimie de Strasbourg, CNRS et Université de Strasbourg, UMR 7177, Laboratoire de Synthèses Métallo-Induites, 4 rue Blaise Pascal, CS 90032, 67081 Strasbourg Cedex, France. E-mail: barloy@unistra.fr*
[b]*Laboratory of Molecular Catalysis, Institute of Chemistry/UFRGS, Av. Bento Gonçalves 9500, Porto Alegre, RS, 91501-970, Brazil*
[c]*Laboratory of New Organic Materials, Institute of Chemistry/UFRGS, Av. Bento Gonçalves 9500, Porto Alegre, RS, 91501-970, Brazil. E-mail: rodembusch@iq.ufrgs.br*

† Electronic supplementary information (ESI) available. CCDC reference numbers 821838 and 821839. For ESI and crystallographic data in CIF or other electronic format see DOI: 10.1039/c1dt10666j

Results and discussion

The synthesis of ligands **1a** and **1b** has been reported by our research group.[27,28] Initially, 4-(*p*-methoxyphenyl)-7-bromo-2,1,3-benzothiadiazole **1c** was isolated as a by-product after preparation of **1b**. Its synthesis was optimized using an equal amount of 4,7-dibromo-2,1,3-benzothiadiazole and 4-methoxyphenylboronic acid.

We prepared complexes **3a–c** *via* the synthetic pathway depicted in Scheme 2, following the procedure reported for the synthesis of an analogous 6-membered palladacyclic derivative of 2-benzylpyridine.[29,30] The use of palladium(II) acetate in acetic acid at 70 °C is known as an efficient cyclopalladation method.[21] Indeed, under these metallation conditions, we isolated and characterized complexes **2a–c** from **1a–c** in good yields (65–77%). These μ-acetato dimeric complexes led then to cyclopalladated μ-chloro dimers upon reaction with lithium chloride in acetone at room temperature. The latter species were not isolated, and were immediately submitted to reaction with pyridine in dichloromethane at room temperature to afford the monomeric pyridine-coordinated complexes **3a–c**. Compounds **3a–c** latter were characterized by ^{1}H and $^{13}C\{^{1}H\}$ NMR, and elemental analysis.

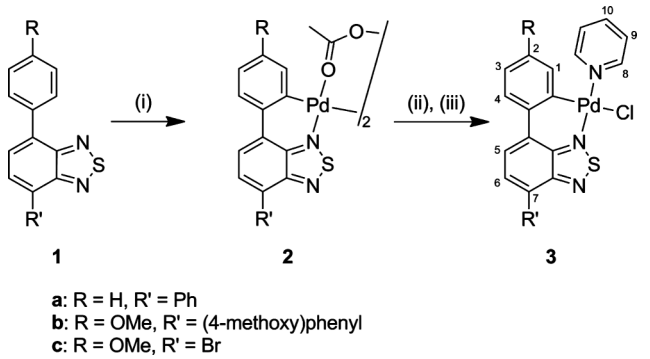

Scheme 2 Synthesis of cyclopalladated benzothiadiazoles. (i) $Pd(OAc)_2$, AcOH, 70 °C. (ii) LiCl, acetone, RT. (iii) Pyridine, CH_2Cl_2, RT.

Incidentally, an attempt at double cyclopalladation of **1b** using two equivalents of $Pd(OAc)_2$ was unsuccessful, leading only to the monocyclopalladated complex **2b**. This is actually not surprising as the remaining nitrogen atom of the thiadiazole ring is probably less prone to coordinate to a second palladium atom, thus obviously preventing the cyclopalladation of the other phenyl ring. Overall the synthesized palladium complexes were stable enough to be completely characterized.

The sulfur atom did not interfere with the cyclometallation process by coordinating to palladium. The stretching carboxylate absorptions in the infrared spectra of **2a–c**, at 1410–1444 cm^{-1} and 1556–1570 cm^{-1}, are characteristic of bridging acetato ligands.[31,32] In their ^{1}H NMR spectra, the only methyl signal of the μ-acetato ligands appears as a singlet at *ca.* 2.3 ppm, which implies that both methyl groups are magnetically equivalent in a *transoid* stereochemistry of the dimer.[18,29,33] Concerning the pyridine-coordinated complexes **3a–c** stereochemistry, we anticipated that the pyridine ligand would be located *trans* with regard to the thiazole ligand because of the antisymbiotic effect.[34] It is indeed the case, as revealed by an important shielding of proton H1 (δ 5.97–6.53 ppm) by the anisotropy cone of pyridine, in analogy with reported parent cyclopalladated complexes.[25,35–37]

Crystal structures

The molecular structures of compounds **2c** and **3c** are shown in Fig. 1 and 2, with selected bond distances and angles. Those are the first reported X-ray structures of *N*-coordinated palladium 2,1,3-thiadiazole complexes. The structure of the binuclear complex **2c** includes a C_2 symmetry axis. Both palladium complexes adopt a classical distorted square-planar geometry; Pd and the four coordinating atoms are coplanar (± 0.08 Å). Within the 6-membered palladacycles, N1, C1, C6, C7 and C12 are almost coplanar (± 0.02 Å); the Pd1–C12 bond distances lie in the normal range, and the Pd1–N1 bond distances are close to the values found for palladium imidazole complexes.[38] Within the BTD ligand, the N1–S1 bond is longer than the N2–S2 bond by 0.045–0.048 Å, as an effect of the bonding of N1 to Pd1. This is an indication of the diminished double bond character[39] of the nitrogen–sulfur bond in the thiazole heterocycle.

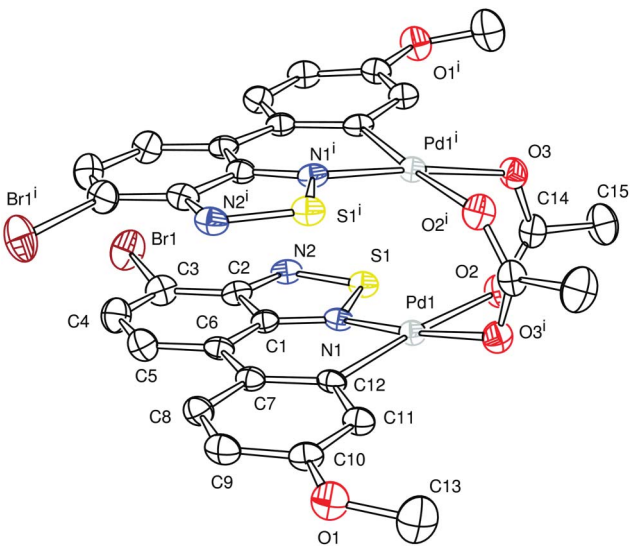

Fig. 1 Ortep plot of compound **2c**. Thermal ellipsoids are drawn at 50% probability level. Hydrogen atoms and CH_2Cl_2 have been omitted for clarity. Selected bond lengths [Å] and bond angles [deg]: Pd1–C12 1.992(4), Pd1–N1 1.989(3), Pd1–O2 2.165(3), Pd1–$O3^{i}$ 2.064(3), S1–N1 1.647(3), S1–N2 1.599(4), C1–N1 1.338(5), C2–N2 1.350(5), N1–Pd1–C12 90.55(15), N1–Pd1–O2 90.54(12), C12–Pd1–$O3^{i}$ 93.24(14), C1–N1–Pd1 128.7(3), C7–C12–Pd1 126.0(3), N1–S1–N2 98.67(18), S1–N1–C1 108.6(3), S1–N2–C2 107.3(3), N1–C1–C2 110.8(3), N2–C2–C1 114.6(4).

The *transoid* stereochemistry of complex **2c** that had been revealed by NMR analysis (*vide supra*) is confirmed by its X-ray structure. It shows several structural similarities with recently reported binuclear 6-membered palladacyclic complexes:[37,40] an "open-book" shape, with a dihedral angle of 23.93° between the palladium coordination planes; a Pd···Pd distance [2.9026(6) Å] shorter than the sum of the van der Waals radii; significantly different palladium–oxygen bonds [2.165(3) *vs.* 2.064(3) Å], because of the *trans* influence of the carbanionic ligand; a bite angle (N1–Pd1–C12) close to 90°. We also observe that the mean planes of the aromatic rings of the BTD ligands are

Table 1 UV-Vis absorption data from the complexes **2a–c** and **3a–c** in solution

Comp.	Solvent	Conc. ($\times 10^{-5}$ M)	λ_{abs} (nm), (ε, $M^{-1}cm^{-1}$)	Solvatochromism[a]	
				Low energy band (λ_2)	High energy band (λ_1)
2a	CH_2Cl_2	4.76	299 (19496), 470 (6282)	6	2
	Acetonitrile		297 (20462), 464 (6576)		
2b	CH_2Cl_2	1.73	306 (19306), 509 (5780)	10	8
	Acetonitrile		298 (19320), 499 (6185)		
2c	CH_2Cl_2	3.29	300 (18359), 333 (sh), 506 (6809)	16	5
	Acetonitrile		285 (sh), 329 (sh), 490 (3769)		
3a	CH_2Cl_2	1.82	297 (21311), 333 (sh), 463 (7268)	5	3
	Acetonitrile		294 (15859), 329 (sh), 458 (5286)		
3b	CH_2Cl_2	3.68	303 (13505), 497 (4348)	7	7
	Acetonitrile		296 (14973), 490 (4647)		
3c	CH_2Cl_2	4.58	290 (sh), 316 (sh), 332 (sh), 491 (2402)	4	2
	Acetonitrile		288 (sh), 314 (sh), 329 (sh), 487 (1943)		

(sh) shoulder[a] Solvatochromism in the ground state

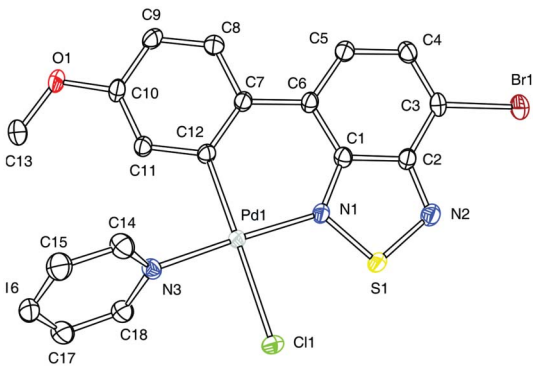

Fig. 2 Ortep plot of compound **3c**. Thermal ellipsoids are drawn at 50% probability level. Hydrogen atoms have been omitted for clarity. Selected bond lengths [Å] and bond angles [deg]: Pd1–C12 2.015(2), Pd1–N1 1.9938(19), Pd1–N3 2.0376(19), Pd1–Cl1 2.4115(6), S1–N1 1.6499(19), S1–N2 1.605(2), C1–N1 1.341(3), C2–N2 1.343(3), N1–Pd1–C12 90.43(8), N1–Pd1–Cl1 89.98(6), C12–Pd1–N3 92.61(8), C1–N1–Pd1 128.71(15), C7–C12–Pd1 125.54(16), N1–S1–N2 98.23(10), S1–N1–C1 108.68(15), S1–N2–C2 108.41(16), N1–C1–C2 111.02(19), N2–C2–C1 113.7(2).

parallel and distant by *ca.* 3.4 Å, suggesting some aromatic π–π stacking.

The X-ray structure of **3c** confirms that the pyridine ligand coordinates the palladium ion *cis* to the Pd–C bond. The pyridine is bent with respect to the coordination plane by 63.67°. The Pd1–C12 bond distance is in the normal range, but the Pd1–Cl1 bond is markedly long [2.4115(6) Å];[38] this is explained by the high *trans* influence of the methoxyphenyl ligand, as in complex **2c**.

Absorption spectra

Electronic spectra in solution of the Pd complexes have been recorded in the 700–200 nm range in dichloromethane and acetonitrile at room temperature and their corresponding photophysical data are gathered in Table 1. The UV-Vis spectra of the complexes showed in both solvents absorption bands between ~300 nm (λ_1) and ~500 nm (λ_2) (Fig. 3). The observed bands in the absorption spectrum are assigned to spin-allowed transitions from the singlet ground state to singlet excited states according the relatively high molar extinction coefficients. The first band (λ_1) locates at around 300 nm and can be probably assigned to ligand-localized (LC)

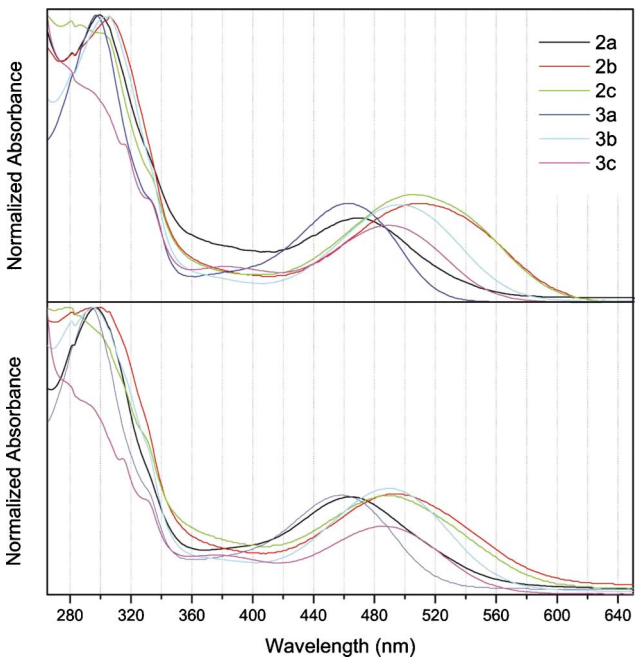

Fig. 3 Electronic absorption spectra of dimeric **2a–c** and monomeric **3a–c** complexes in solution at room temperature: dichloromethane (top) and acetonitrile (bottom).

states due to intraligand π–π* transitions of the BTD ligands, with high molar extinction coefficients ($\varepsilon \sim 10^4$ $M^{-1}cm^{-1}$). Concerning the ligand absorption bands location,[23] these observed blue shifted bands can feature to metal-perturbed LC transitions, which are slightly influenced by changing the auxochrome groups in the ligand structure.[41]

The second set of less intense ($\varepsilon \sim 10^3$ $M^{-1}cm^{-1}$) absorption bands (λ_2) can be observed located at lower energies, at 463–506 nm and 458–499 nm for dichloromethane and acetonitrile, respectively and probably result from a transition involving the palladacycle.[42] The extinction coefficients in this region are larger than expected for a d–d transition and by virtue of this it was eliminated ligand-field excited states as an explanation for these absorption bands. In this way, these less intense low-energy absorptions are tentatively ascribed as metal-to-ligand charge

transfer (^{1}MLCT) character.[43] These transitions are commonly observed in organometallic complexes because of the low-valent nature of the metal center and low-energy position of the orbitals in many ligands, as presented in BTD. Analogous to classical coordination compounds MLCT transitions are typically intense ($\varepsilon = 10^3$-10^4 $M^{-1}cm^{-1}$) and solvent dependent, as observed in these complexes. Concerning the dimeric complexes, it could be expected some metal-to-metal charge transfer (MMCT) states, which arises from electronic transitions between metal-centered orbitals of two or more metals. These bands are typically present in the blue or near-ultraviolet regions, and their energies are normally not dependent on the solvent. However, the observed solvatochromic effect, as well as the domination of the low energy absorption bands in the visible region, allows us to discard such character.[44]

Any significant difference could be observed between the monomeric and dimeric Pd complexes, since it was already observed that extinction coefficients for the dimer complexes are substantially larger than for the monomeric derivatives.[45] It is worth mentioning that both sets of absorption bands are solvent dependent, where a negative solvatochromic effect of ~8 nm and ~4.5 nm could be observed for the low (λ_2) and high energy bands (λ_1), respectively (Table 1). The negative solvatochromic effect observed in the low energy absorption bands is probably due to the higher dipole moment in the ground state due to ^{1}MLCT character, since in similar Pt complexes the same photophysical behavior could be observed, where the solvent can relax around the ground state prior to excitation. This will lower the energy of the ground state, resulting in a blue shifted absorption.[46,47] Concerning the dimeric complexes, the UV-Vis absorption spectra of **3a–c** follow Beer's law, indicating that aggregation does not occur at concentrations below ~50 μM.[48]

DRUV spectra

Fig. 4 presents the diffuse reflectance UV-Vis absorbance and diffuse reflectance obtained from the Pd complexes in the solid state, which display notable differences with those obtained in solution, as has been already observed in cyclopalladated complexes.[43] All complexes present a strong decrease of the diffuse reflectance from the near-infrared to the visible region, which is related to the observed red–orange colours for the complexes, and can be probably attributed to a combination of ^{1}MLCT (or even ^{1}MMLCT to dimeric complexes) and π–π* transitions, due to Pd···Pd and π stacking interactions.[49]

It can be observed that complexes **2a–c** present a higher diffuse reflectance percentage in the visible region, in contrast to complexes **3a–c**, which present a lower one. This photophysical behavior indicates that the bridge ligands acetate in the dimeric complexes and the ancillary ligands in the monomeric complexes are probably tailoring the absorption in the visible region in the solid state. On the other hand, complexes **2a–c** present a major contribution to the near-infrared region band, since a decrease of the diffuse reflectance of 50–70% can be observed. A strong absorption in the visible–NIR region can be observed for the complexes. Concerning the solution results, the lower wavelength bands cannot be associated with the benzothiadiazole ligand absorption, since its absorption maxima are ascribed to be located at around 300 nm in solution. Additional red-shifted bands located from 500 nm up to 700 nm, which depend on the electronic

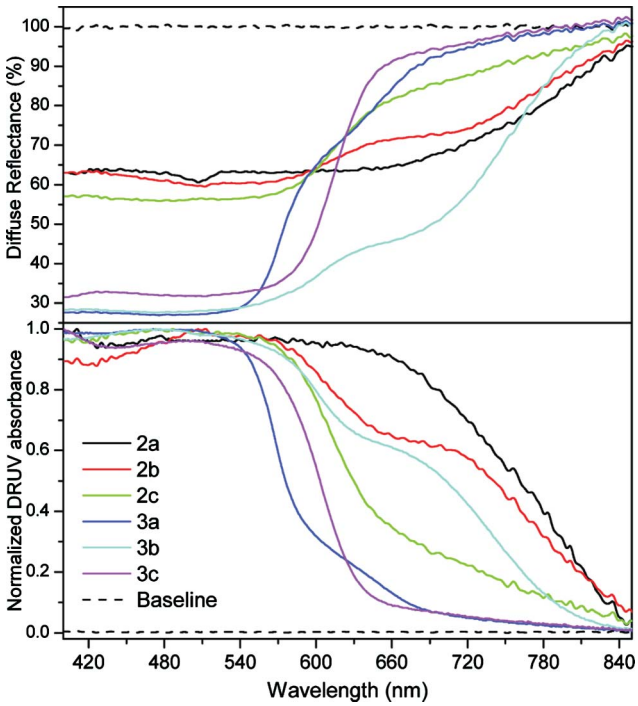

Fig. 4 Diffuse reflectance (top) and normalized DRUV absorbance (bottom) for the complexes **2a–c** and **3a–c**.

Table 2 Solid-state absorption data of the cyclopalladated complexes

Pd Complex	λ_{max}^{abs}(nm)	E_g^{opt} (eV)
2a	652	1.90
2b	695	1.78
2c	692	1.79
3a	619	2.00
3b	667	1.86
3c	526	2.35

structure of the complexed metal, are present, which can probably be attributed to the metal–ligand interaction. The ancillary ligands in the palladium complexes seem to play a fundamental role in the absorption spectra, only when an additional chromophore (aryl) is present in the benzothiadiazole moiety. The dimeric palladium complex (**2a**) presents a higher absorption in the near infrared region when acetate is used as secondary ligand. In the monomeric complex (**3a**), this electronic absorption is practically absent. The dimeric **2c** and monomeric **3b** complexes present a similar behavior, where two main bands can be observed located at 550 nm and 700 nm, indicating that the R and R′ moieties are playing a fundamental role in the absorption spectra. No significant near-infrared band can be observed to the complexes **2c** and **3c**, where the organic moieties of the benzothiadiazole seem again to be decisive in the absorption bands. The palladium complexes in Fig. 4 presents only methoxy and bromine groups, which do not allow a higher conjugation of the benzothiadiazole ligand. Additionally, the solid-state absorbance spectra allowed us to determine the optical band gaps from the palladium complexes (E_g^{opt}) (Table 2). These values lies in the range 1.78–2.35 eV and are in agreement with those of similar palladium complexes.[22]

Table 3 Fluorescence emission data from the complexes **2a–c** and **3a–c** in solution[a]

Comp.	Solvent	$^1\lambda_{em}$ (nm)/$^2\lambda_{em}$ (nm)	Solvatochromism[b]		Stokes shift $\Delta\lambda_{ST}$ (cm^{-1})	
			Low energy band	High energy band	Low energy band	High energy band
2a	CH_2Cl_2	370*, 474/564	7	8	3546	12347
	Acetonitrile	356*, 482/571			4038	12924
2b	CH_2Cl_2	353*, 524/604	7	15	3090	13596
	Acetonitrile	356*, 539/611			3674	15005
2c	CH_2Cl_2	353*, 519/557	12	20	1809	14066
	Acetonitrile	356*, 539/545			2060	16535
3a	CH_2Cl_2	386*, 488/562	68	5	3805	13179
	Acetonitrile	354*, 556/567			4198	16028
3b	CH_2Cl_2	398*, 540/615	8	11	3860	14485
	Acetonitrile	356*, 548/626			4434	15535
3c	CH_2Cl_2	388*, 521/583	21	25	3214	15289
	Acetonitrile	354*, 542/558			2612	16272

[a] $^1\lambda_{em}$: emission maxima using excitation λ_1 (data from UV-Vis spectra). $^2\lambda_{em}$: emission maxima using excitation λ_2 (data from UV-Vis spectra). The asterisk indicates additional blue shifted bands. [b] Solvatochromism in the excited state measured only for the maxima bands in each emission regions.

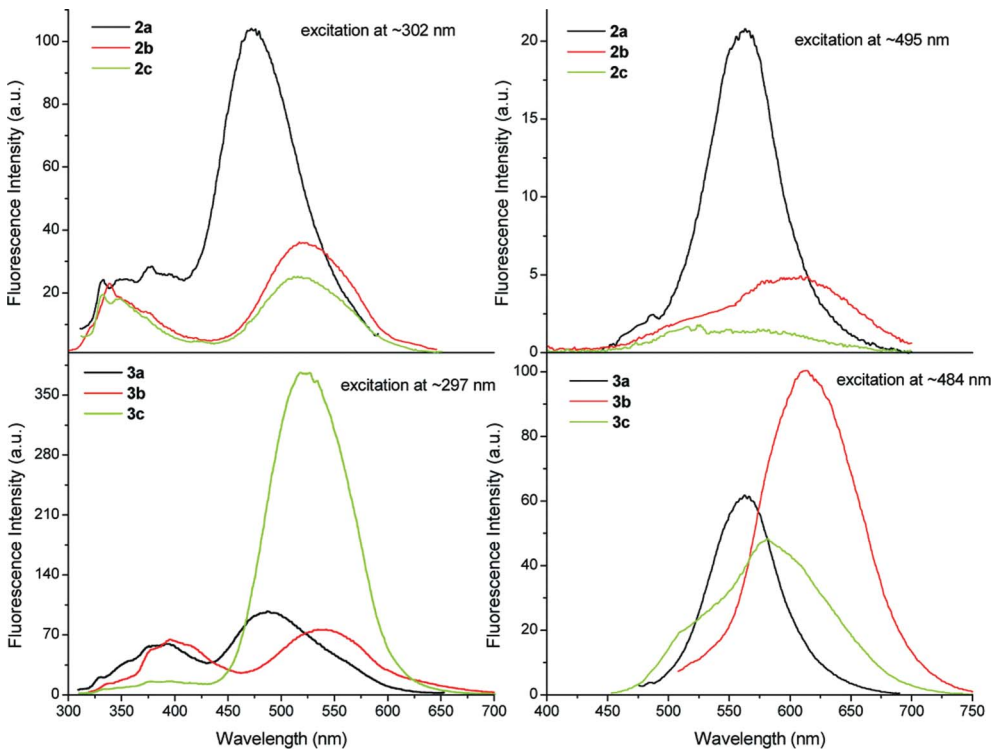

Fig. 5 Emission spectra at room temperature of the dimeric **2a–c** and monomeric **3a–c** Pd complexes in dichloromethane. The spectra were obtained using λ_1 and λ_2 as excitation wavelengths (data from UV-Vis spectra).

Emission spectra

All the palladium complexes under study show appreciable emission in the visible region of the spectrum at room temperature, as can be observed in Fig. 5 and 6. The relevant fluorescence emission data are summarized in Table 3. According to the literature, the luminescence emission from Pd complexes can be attributed to ligand-localized (LC) states due to intraligand π–π* transitions of the ligands, MLCT (monomeric) or MMLCT (dimeric) transitions.[50–54]

The emission spectra were obtained using excitation wavelengths from the UV-Vis data. The measurements in dichloromethane were performed using excitation and emission slits of 5.0 nm/5.0 nm, respectively to the monomeric complexes. In order to increase the ratio signal : noise a different emission slit (3.0 nm) was applied to the dimeric complexes. In acetonitrile a set of slits was used of dimensions 5.0 nm/3.0 nm and 5.0 nm/10.0 nm for the excitation at λ_1 and λ_2 respectively.

It could be observed that the fluorescence emission can be tailored by the excitation wavelength, where excitations at high energy wavelengths allow emissions in the blue–green region (Fig. 5 and 6, left side). On the other hand, a low energy excitation led to emissions in the green–yellow–orange regions (Fig. 5 and 6, right side). For all studied complexes a significant

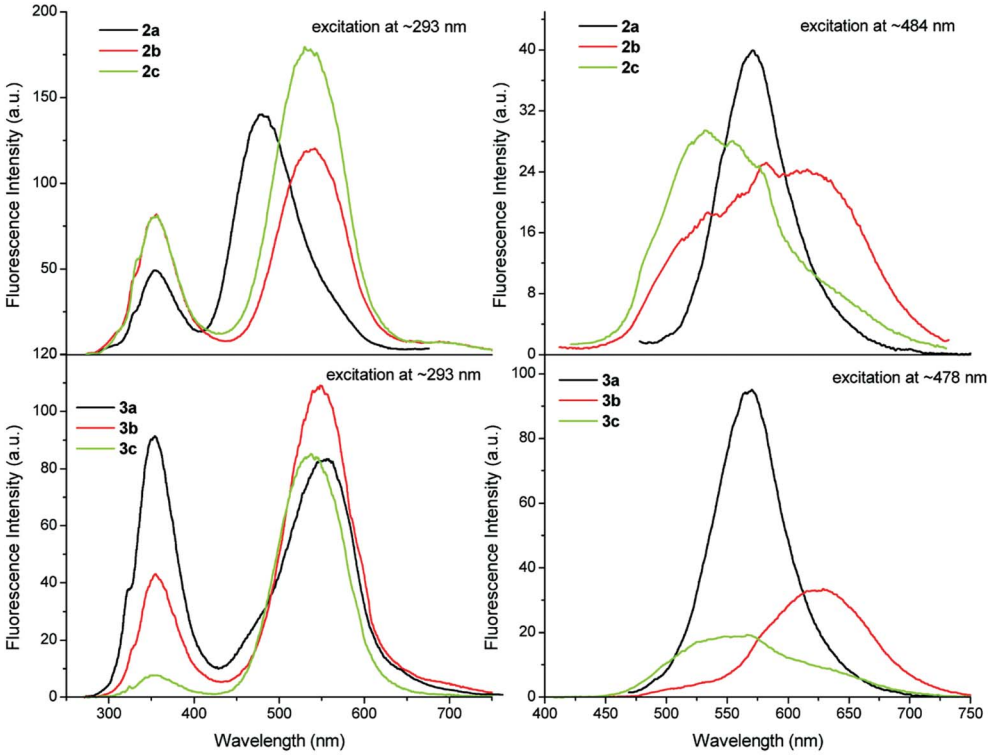

Fig. 6 Emission spectra at room temperature of the dimeric **2a–c** and monomeric **3a–c** Pd complexes in acetonitrile. The spectra were obtained using λ_1 and λ_2 as excitation wavelengths (data from UV-Vis spectra).

solvatochromic effect could be observed in the excited state (Table 3). This behaviour can be attributed to the large ground-state dipole moment[55,56] or could be due to a change in the dipolar or polarization interaction between the ground and the excited-state, where the solvent dipolar and polarization effects are changed much less on going from the ground to the excited state.[57–60] However, the observed negative solvatochromism can normally be attributed to the fact that the transition moment of the main (*z*-polarized) component of the MLCT transition lies antiparallel, where the dipole moment in the excited states is thus much reduced compared to the ground state or may even reverse its direction.[61–64]

The Pd complexes present a fluorescence quantum yield range of 0.004–0.03, where no significant changes could be observed based on the nature of the substituents. Additionally, the dimeric complexes presented higher fluorescence quantum yields compared to the monomeric ones. The compounds present low quantum yields of fluorescence when compared to the free ligands, but these values are better than the majority of cyclopalladated complexes reported so far.[23–26] (For individual fluorescence quantum yield results see the supporting information†).

The first set of fluorescence bands (Fig. 5 and 6, left side) indicates that the emission arises from π–π* ligand-localized singlet state, since the location of the maxima are similar to those observed to the free ligand in solution (493–526 nm).[27] In addition, the obtained excitation spectra monitored at these wavelengths can be related only to the ligand (Fig. S1–S12†), where no emission band related to the complexes can be observed. To the best of our knowledge, no dual fluorescence was ascribed to an emission with this character, which indicates that BTD plays a fundamental role in the π–π* ligand-localized singlet state photophysics. The observed bathochromic shifted band (~350 nm) can be probably related to a locally excited chromophore, metal-perturbed but with a less CT character. The second set of fluorescence emissions (Fig. 5 and 6, right side) present one main band located at around 580 nm, probably due to ^{1}MLCT (monomeric) or ^{1}MMLCT (dimeric) excited states with a strong CT character. The dimeric and monomeric complexes present a similar behavior in the fluorescence emission, with the R and R′ moieties again playing a fundamental role in the photophysics. Additionally, the complexes **2b** and **3b** present a higher fluorescence emission wavelength probably due to their more extended conjugation, due to the ligand moieties, as expected. The same photophysical behaviour could be detected when acetonitrile was used as the solvent. Excitation spectra of the complexes (see Fig. S1–S12 in the supporting information†) were also performed in both solvents dichloromethane and acetonitrile in order to study the emissive species in the excited state and also the presence of some free ligand in the solution. The presence of some small impurity was ignored since the excitation spectra in dichloromethane observed at the long emission wavelength presents a band maximum, which matches the obtained UV-Vis maxima of the complexes (red shifted band), as expected. On the other hand, it could also be observed that the excitation spectra observed at the short emission wavelength presents only an excitation band maximum located at around 370 nm. A red shifted band (over 400 nm) related to the complex (MLCT band) was not observed, which indicates that the fluorescence emission observed under excitation at the high energy absorption band is due to ^{1}LC transitions located in the BTD ligands. The excitation spectra monitored with different emission wavelengths and its comparison with the absorption spectra

suggest that there are two competitive pathways for deactivation of the higher-energy, as already observed in similar Pd complexes.[48] Furthermore, the location of the excitation maxima monitored at the short emission wavelength, ascribed to a ligand emission character suggests the free ligand is not present in solution, since absorption maxima higher than 420 nm are found for the free ligand.[27] The same photophysical behaviour could be observed in acetonitrile, however the band ascribed to the complex seems to be more affected by this solvent, since the maxima between the excitation and the absorption spectra do not match very well, which probably indicates that the solvent coordinates the complex. No fluorescence emission could be observed in the solid-state from the palladium complexes. Although the photophysical mechanism which leads to the lack of fluorescence is unclear, different processes could take place, such as ligand–ligand interaction (π stacking is already present in the ground state)[65–68] or the presence of thermally accessible metal-centered (MC) excited states, the geometry of which is strongly distorted with respect to that of the ground state, leading to the rapid deactivation of the excited luminescent state.[69–70]

Conclusions

We have reported in this paper the unprecedented cyclopalladation of benzothiadiazole derivatives, their complete characterization and the study of their light-emitting properties. The 4,7-diaryl-2,1,3-benzothiadiazoles **1a** and **1b**, and the newly synthesized 4-(*para*-methoxyphenyl)-7-bromo-2,1,3-benzothiadiazole **1c**, were smoothly cyclopalladated to yield the dimeric, μ-acetato complexes **2a–c**. C–H activation took place at the *ortho* position of the 4-aryl group after coordination of one of the nitrogen atoms, leading to a six-membered palladacycle. The dimers **2a–c** were converted into the cyclopalladated monomeric complexes **3a–c** through well-known synthetic pathways. Analysis of the complexes in solution by NMR and, for some of them, in the solid state by X-ray crystallography, provided valuable structural information: *transoid* geometry of **2a–c**, and *cis* coordination of the pyridine ligand with regard to the Pd–C bond in **3a–c**. All the complexes present intense absorption at around 300 nm *via* ^{1}LC transitions located in BTD ligands, and additional low energy absorption bands, higher than 450 nm with a ^{1}MLCT character. The complexes are fluorescent in solution at room temperature, where two emission bands could be observed, a high energy band, ascribed to the ligand emission and an additional red shifted low intense band due to the complex emission. Both fluorescence bands indicate CT character due to a strong solvatochromic effect in the excited state.

Experimental

General

Experiments were carried out under an argon atmosphere using a vacuum line. Solvents were dried by standard methods and distilled under argon, except acetic acid. All reagents were purchased from Acros, Aldrich and Alfa Æsar and used without further purification. The Suzuki coupling catalyst precursor (PCN palladacycle),[18,71] 4,7-dibromo-2,1,3-benzothiadiazole[27] and compounds **1a,b**[27] were prepared according to the literature. FT-IR spectra were recorded on a Nicolet IR200 spectrometer. NMR spectra were obtained at room temperature on Bruker Avance spectrometers. ^{1}H NMR spectra were recorded at 300.13 MHz and referenced to $SiMe_4$. $^{13}C\{^1H\}$ NMR spectra (broadband decoupled) were recorded at 75.48 MHz or 125.7 MHz and referenced to $SiMe_4$. The NMR assignments were supported by COSY, HSQC and/or HMBC spectra. For the adopted numbering scheme, see Scheme 2. Multiplicity: s = singlet, d = doublet, t = apparent triplet, m = multiplet. Fluorescence and excitation spectra were measured with a Shimadzu spectrofluorometer RF5301. The UV-Vis data in solution was obtained with a spectrophotometer Shimadzu UV2450PC. The diffuse reflectance spectra were measured using an ISR-2200 Integrating Sphere Attachment. For these experiments in the solid state, the palladium complexes were treated as powder. The experiments were performed at room temperature and the baseline in the solid-state was obtained using $BaSO_4$ (Wako Pure Chemical Industries, Ltd.). The quantum yields of fluorescence (ϕ_{fl}) were determined at 25 °C in dichloromethane solutions using the optically dilute method (absorbance lower than 0.05) and Rhodamine 6G (0.95) and Rhodamine 110[72] (0.92) in ethanol as quantum yield standards.[73,74]

Synthesis of compound 1c

A Schlenk tube was charged with CsF (258 mg, 1.70 mmol), 4-methoxyphenylboronic acid (258 mg, 1.70 mmol) and the PCN palladacyclic catalyst (7 mg, 17 μmol). A solution of 4,7-dibromo-2,1,3-benzothiadiazole (500 mg, 1.70 mmol) in 1,4-dioxane (5 mL) was added. The reaction mixture was stirred at 130 °C for 3 days. The solution was then allowed to cool to room temperature and the solvent evaporated under reduced pressure. The crude material was chromatographed on silica gel (Merck, 40–63 μm) using pentane: Et_2O (100 : 1) as eluent. Compound **1c** was isolated as a yellow powder (420 mg, 77% yield). ^{1}H RMN (300 MHz, $CDCl_3$): δ = 7.90 (d, $^3J_{HH}$ = 7.7 Hz, 1H, H_{BTD}), 7.86 (d, $^3J_{HH}$ = 8.8 Hz, 2H, H_{Ph}), 7.52 (d, $^3J_{HH}$ = 7.9 Hz, 1H, H_{BTD}), 7.06 (d, $^3J_{HH}$ = 8.8 Hz, 2H, H_{Ph}), 3.89 (s, 3H, OMe) ppm. $^{13}C\{^1H\}$ RMN (75.5 MHz, $CDCl_3$): δ = 160.1, 153.9, 153.2, 133.6, 132.3, 130.4, 129.0, 127.4, 114.2, 112.2, 55.4 ppm. Anal. calcd for $C_{13}H_9BrN_2OS$ (321.20): C 48.61, H 2.82, N 8.72. Found: C 48.31, H 2.85, N 8.87.

General procedure for the synthesis of compounds 2a–c

Compound **1a–c** (1.04 mmol; **1a**: 300 mg, **1b**: 362 mg, **1c**: 334 mg) was dissolved in AcOH (10 mL) in a Schlenk tube and $Pd(OAc)_2$ (233 mg, 1.04 mmol) was added. The reaction was stirred at 70 °C for 1 h and product **2a–c** precipitated. The reaction mixture was allowed to cool to room temperature. The precipitate was collected on a frit and washed with small amounts of AcOH, and then with Et_2O and pentane. The resulting powder was dried under vacuum.

2a: orange powder, 361 mg, 77% yield. IR (neat): $\tilde{\nu}$ = 1556 and 1444 cm^{-1}. ^{1}H RMN (300 MHz, $CDCl_3$): δ = 7.85 (d, $^3J_{HH}$ = 7.1 Hz, 2H, $H_{Ph\ ortho}$), 7.63–7.46 (m, 5H, H_{Ar}), 7.33 (m, 1H, H-1 or H-4), 7.19 (m, 1H, H-4 or H-1), 6.93–6.83 (m, 2H, H-2 + H-3), 2.33 (s, 3H, OAc) ppm. Anal. calcd for $C_{40}H_{28}N_4O_4Pd_2S_2$, H_2O (923.67): C 52.01, H 3.27, N 6.07; Found: C 52.41, H 3.64, N 5.64.

2b: burgundy red powder, 349 mg, 65% yield. IR (neat): $\tilde{\nu}$ = 1570 and 1414 cm^{-1}. ^{1}H RMN (300 MHz, $CDCl_3$): δ = 7.84 (d, $^3J_{HH}$ = 8.8 Hz, 2H, Ar-7), 7.49 (d, $^3J_{HH}$ = 7.7 Hz, 1H, H-5), 7.40 (d, $^3J_{HH}$ = 7.7 Hz, 1H, H-6), 7.11 (m, 3H, H-4 + Ar-7), 6.90 (d, $^4J_{HH}$ = 2.7 Hz,

1H, H-1), 6.49 (dd, $^3J_{HH}$ = 8.8 Hz, $^4J_{HH}$ = 2.6 Hz, 1H, H-3), 3.94 (s, 3H, OMe-7), 3.80 (s, 3H, OMe-2), 2.33 (s, 3H, OAc) ppm. Anal. calcd for $C_{44}H_{36}N_4O_8Pd_2S_2$, $2H_2O$ (1061.80): C 49.77, H 3.80, N 5.28; Found: C 50.01, H 3.64, N 5.41.

2c: red powder, 389 mg, 77% yield. IR (neat): $\tilde{\nu}$ = 1559 and 1410 cm^{-1}. ^{1}H RMN (300 MHz, $CDCl_3$): δ = 7.64 (d, $^3J_{HH}$ = 8.1 Hz, 1H, H-6), 7.29 (d, $^3J_{HH}$ = 8.1 Hz, 1H, H-5), 7.16 (d, $^3J_{HH}$ = 9.0 Hz, 1H, H-4), 6.78 (d, $^4J_{HH}$ = 2.6 Hz, 1H, H-1), 6.57 (dd, $^3J_{HH}$ = 8.8 Hz, $^4J_{HH}$ = 2.7 Hz, 1H, H-3), 3.82 (s, 3H, OMe), 2.31 (s, 3H, OAc) ppm. ^{13}C{^{1}H} RMN (125.7 MHz, $CDCl_3$): δ = 183.2, 157.4, 152.1, 144.9, 136.6, 133.1, 131.6, 123.3 (2 signals), 120.6, 117.5, 112.7, 111.6, 55.3, 24.2 ppm. Anal. calcd for $C_{30}H_{22}Br_2N_4O_6Pd_2S_2$ (971.30): C 37.10, H 2.28, N 5.77; Found: C 37.01, H 2.49, N 5.60.

General procedure for the synthesis of compounds 3a–c

Compound **2a–c** (0.398 mmol; **2a**: 361 mg, **2b**: 408 mg, **2c**: 387 mg) was dissolved in acetone (10 mL) in a Schlenk tube. Lithium chloride (34 mg, 0.796 mmol) was added and the reaction mixture was stirred for 1 h at room temperature. The resulting solid was filtered and dried under vacuum. It was then partly dissolved in CH_2Cl_2 (10 mL) in a Schlenk tube, and pyridine (63 mg, 0.796 mmol) was added. The suspension was stirred at room temperature for 1 h, and the resulting solid collected on a frit and dried under vacuum. The product was recrystallized in dichloromethane.

3a: orange powder, 149 mg, 37% yield.^{1}H RMN (300 MHz, $CDCl_3$): δ = 8.93 (d, $^3J_{HH}$ = 4.9 Hz, 2H, H-8), 8.37 (d, $^3J_{HH}$ = 7.7 Hz, 1H, H-5), 8.00–7.81 (m, 5H), 7.62–7.38 (m, 5H), 7.20 (ddd, $^3J_{HH}$ = 8.2 Hz, $^3J_{HH}$ = 7.0 Hz, $^4J_{HH}$ = 1.3 Hz, 1H, H-3), 6.85 (ddd, $^3J_{HH}$ = 8.2 Hz, $^3J_{HH}$ = 6.6 Hz, $^4J_{HH}$ = 1.5 Hz, 1H, H-2), 6.53 (dd, $^3J_{HH}$ = 8.1 Hz, $^4J_{HH}$ = 1.1 Hz, 1H, H-1) ppm ^{13}C{^{1}H} RMN (125.7 MHz, $CDCl_3$): δ = 153.4, 151.4, 146.8, 142.1, 138.2, 137.4, 135.8, 133.0, 132.4, 131.7, 129.1, 128.9, 128.7 (2 signals), 127.5, 126.0, 125.4, 125.3, 124.8 ppm. Anal. calcd for $C_{23}H_{16}ClN_3PdS$, H_2O (526.35): C 52.48, H 3.45, N 7.98. Found C 52.23, H 3.65, N 7.65.

3b: reddish–brown powder, 330 mg, 73% yield. ^{1}H RMN (300 MHz, $CDCl_3$): δ = 8.96 (d, $^3J_{HH}$ = 4.9 Hz, 2H, H-8), 8.22 (d, $^3J_{HH}$ = 7.9 Hz, 1H, H-5), 7.96–7.86 (m, 3H, Ar-7 + H-10), 7.83 (d, $^3J_{HH}$ = 8.8 Hz, 1H, H-4), 7.77 (d, 1H, $^3J_{HH}$ = 7.7 Hz, 1H, H-6), 7.44 (t, $^3J_{HH}$ = 6.4 Hz, 2H, H-9), 7.08 (d, $^3J_{HH}$ = 8.8 Hz, 2H, Ar-7), 6.78 (dd, $^3J_{HH}$ = 8.6 Hz, $^4J_{HH}$ = 2.6 Hz, 1H, H-3), 6.00 (d, $^4J_{HH}$ = 2.6 Hz, 1H, H-1), 3.90 (s, 3H, OMe-7), 3.53 (s, 3H, OMe-2) ppm. ^{13}C{^{1}H} RMN (125.7 MHz, $CDCl_3$): δ = 160.1, 157.6, 153.6, 152.5, 146.7, 143.0, 139.2, 132.2, 131.6, 131.0, 129.1, 128.7, 126.2, 126.1, 125.8, 125.2, 122.8, 114.5, 111.8, 55.1, 54.9 ppm. Anal. calcd for $C_{25}H_{20}ClN_3O_2PdS$, H_2O (586.41): C 51.21, H 3.78, N 7.17. Found C 50.72, H 3.98, N 6.87.

3c: red powder, 182 mg, 42% yield. ^{1}H RMN (300 MHz, $CDCl_3$): δ = 8.93 (d, $^3J_{HH}$ = 4.9 Hz, 2H, H-8), 8.00 (d, $^3J_{HH}$ = 8.1 Hz, 1H, H-5), 7.91 (d, $^3J_{HH}$ = 8.1 Hz, 1H, H-6), 7.88 (t, $^3J_{HH}$ = 8.0 Hz, 1H, H-10), 7.77 (d, $^3J_{HH}$ = 8.8 Hz, 1H, H-4), 7.44 (t, $^3J_{HH}$ = 6.6 Hz, 2H, H-9), 6.75 (dd, $^3J_{HH}$ = 8.6 Hz, $^4J_{HH}$ = 2.6 Hz, 1H, H-3), 5.97 (d, $^4J_{HH}$ = 2.6 Hz, 1H, H-1), 3.52 (s, 3H, OMe) ppm. ^{13}C{^{1}H} RMN (125.7 MHz, $CDCl_3$): δ = 158.1, 153.3, 152.1, 146.3, 143.2, 138.3, 133.4, 133.1, 125.4, 125.2, 124.8, 124.2, 122.2, 111.8, 111.3, 54.4 ppm. Anal. calcd for $C_{18}H_{13}BrClN_3OPdS$ (541.16): C 39.95, H 2.42, N 7.76. Found C 40.21, H 2.54, N 7.59.

X-Ray crystallography

Suitable crystals of compounds **2c** and **3c** were respectively obtained as red plates and red prisms by cooling saturated

Table 4 Crystal data and structure refinement for **2c** and **3c**

Compound	**2c**·2CH_2Cl_2	**3c**
Formula	$C_{32}H_{26}Br_2Cl_4N_4O_6Pd_2S_2$	$C_{18}H_{13}BrClN_3OPdS$
Formula weight	1141.11	541.13
Cryst. syst.	Orthorhombic	Triclinic
Space group	*P*bcn	$P\bar{1}$
a/Å	10.8302(2)	8.6025(4)
b/Å	26.1898(5)	10.4897(4)
c/Å	13.3993(2)	10.9885(3)
α (°)	90	77.842(2
β (°)	90	85.148(2)
γ (°)	90	67.469(2)
V/Å^3	3800.59(12)	895.34(6)
Z	4	2
d_c/g cm^{-3}	1.994	2.007
μ/mm^{-1}	3.489	3.546
F(000)	2224	528
Crystal size/mm	0.20 × 0.18 × 0.10	0.30 × 0.25 × 0.20
θ range, deg	1.56 to 30.03	1.90 to 29.99
Index ranges	$-15 \le h \le 10$	$-12 \le h \le 11$
	$-36 \le k \le 34$	$-12 \le k \le 44$
	$-18 \le l \le 18$	$-15 \le l \le 15$
No. of reflns collcd	33822	10301
No. of indep collcd/R_{int}	5558/0.0623	5192/0.0405
Completeness to θ_{max} (%)	99.8	99.6
Data/restrains/params	5558/0/237	5192/0/236
GOF (F^2)	1.182	1.054
$R_1(F)$ ($I > 2\sigma(I)$)	0.0407	0.0292
$wR_2(F^2)$ (all data)	0.1437	0.0740
Largest diff peak/hole, e Å^{-3}	0.900/−1.696	0.584/−1.093

solutions in dichloromethane to 4 °C. The crystals were placed in oil, and a single crystal was selected, mounted on a glass fibre and placed in a low-temperature N_2 stream.

X-Ray diffraction data collection was carried out at 173 K on a Nonius Kappa-CCD diffractometer equipped with an Oxford Cryosystem liquid N_2 device, using Mo-Kα radiation ($\lambda = 0.71073$ Å). The crystal-detector distance was 36 mm. The cell parameters were determined (Denzo software)[75] from reflections taken from one set of 10 frames (1.0° steps in phi angle), each at 20 s exposure. Details of data collection parameters and refinement results are listed in Table 4. The structures were solved by Direct methods using the program SHELXS-97.[76] The refinement and all further calculations were carried out using SHELXL-97.[77] The H-atoms were included in calculated positions and treated as riding atoms using SHELXL default parameters. The non-H atoms were refined anisotropically, using weighted full-matrix least-squares on F^2.

For both complexes, a semi-empirical absorption correction was applied using the MULscanABS routine in PLATON;[78] transmission factors for **2c**: $T_{min}/T_{max} = 0.524/0.662$; transmission factors for **3c**: $T_{min}/T_{max} = 0.351/0.437$.

Acknowledgements

We thank Dr Lydia Brelot for the resolution of the X-ray crystal structures and Mrs Martine Heinrich for technical help. We are grateful to the CNRS for financial support of this work, CAPES-COFECUB for a fellowship granted to FSM (502/05) and Instituto Nacional de Inovação em Diagnósticos para a Saúde Pública (INDI-SAÚDE) for financial support.

References

1 M. T. Lee, C. K. Yen, W. P. Yang, H. H. Chen, C. H. Liao, C. H. Tsai and C. H. Chen, *Org. Lett.*, 2004, **6**, 1241–1244.
2 S. A. Odom, S. R. Parkin and J. E. Anthony, *Org. Lett.*, 2003, **5**, 4245–4248.
3 W. J. Shen, R. Dodda, C. C. Wu, F. I. Wu, T. H. Liu, H. H. Chen, C. H. Chen and C. F. Shu, *Chem. Mater.*, 2004, **16**, 930–934.
4 Q. Hou, Q. Zhou, Y. Zhang, W. Yang, R. Yang and Y. Cao, *Macromolecules*, 2004, **37**, 6299–6305.
5 C. J. Tonzola, M. M. Alam, W. Kaminsky and S. A. Jenekhe, *J. Am. Chem. Soc.*, 2003, **125**, 13548–13558.
6 R. M. F. Batista, S. P. G. Costa and M. M. M. Raposo, *Tetrahedron Lett.*, 2004, **45**, 2825–2828.
7 K. R. Justin Thomas, J. T. Lin, M. Velusamy, Y.-T. Tao and C.-H. Chuen, *Adv. Funct. Mater.*, 2004, **14**, 83–90.
8 X. Zhang, H. Gorohmaru, M. Kadowaki, T. Kobayashi, T. Ishi-i, T. Thiemann and S. Mataka, *J. Mater. Chem.*, 2004, **14**, 1901–1904.
9 Y. N. Kukushkin, S. A. D'yachenko, R. A. Vlasova and N. P. Glazyuk, *Zh. Obshch. Khim.*, 1973, **43**, 1179–1182.
10 B. E. Zaitsev, A. K. Molodkin, V. V. Davydov, M. V. Gorelik and T. K. Gladysheva, *Zh. Neorg. Khim.*, 1980, **25**, 752–760.
11 B. E. Zaitsev, A. K. Molodkin, V. V. Davydov, M. V. Gorelik and T. K. Gladysheva, *Zh. Neorg. Khim.*, 1980, **25**, 1877–1885.
12 B. E. Zaitsev, T. M. Ivanova, V. V. Davydov and A. K. Molodkin, *Zh. Neorg. Khim.*, 1980, **25**, 3031–3036.
13 C. Richardson, P. J. Steel, D. M. D'Alessandro, P. C. Junk and F. R. Keene, *J. Chem. Soc., Dalton Trans.*, 2002, 2775–2785.
14 M. T. S. Ritonga, H. Shibatani, H. Sakurai, T. Moriuchi and T. Hirao, *Heterocycles*, 2006, **68**, 829–836.
15 A. M. A. Alaghaz, *Phosphorus, Sulfur Silicon Relat. Elem.*, 2008, **183**, 2807–2826.
16 J. Albert and J. Granell, *Trends Organomet. Chem.*, 1999, **3**, 99–112.
17 J. Dupont, M. Pfeffer and J. Spencer, *Eur. J. Inorg. Chem.*, 2001, (8), 1917–1927.
18 J. Dupont, C. S. Consorti and J. Spencer, *Chem. Rev.*, 2005, **105**, 2527–2571.
19 A. P. Sadimenko, *Adv. Heterocycl. Chem.*, 2005, **88**, 111–174.
20 *Palladacycles*, ed. J. Dupont and M. Pfeffer, Wiley-VCH, Weinheim, 2008.
21 M. Albrecht, *ibid.*, pp. 13–33.
22 F. Neve, *ibid.*, pp. 285–305 and references cited.
23 M. Ghedini, D. Pucci, G. Calogero and F. Barigelletti, *Chem. Phys. Lett.*, 1997, **267**, 341–344.
24 M. Ghedini, D. Pucci, A. Crispini, I. Aiello, F. Barigelletti, A. Gessi and O. Francescangeli, *Appl. Organomet. Chem.*, 1999, **13**, 565–581.
25 I. Aiello, M. Ghedini and M. La Deda, *J. Lumin.*, 2002, **96**, 249–259.
26 C. S. Consorti, G. Ebeling, F. Rodembusch, V. Stefani, P. R. Livotto, F. Rominger, F. H. Quina, C. Yihwa and J. Dupont, *Inorg. Chem.*, 2004, **43**, 530–536.
27 B. A. D. Neto, A. S. A. Lopes, G. Ebeling, R. S. Gonçalves, V. U. Costa, F. H. Quina and J. Dupont, *Tetrahedron*, 2005, **61**, 10975–10982.
28 F. S. Mancilha, B. A. D. Neto, A. S. Lopes, P. F. Moreira, F. H. Quina, R. S. Gonçalves and J. Dupont, *Eur. J. Org. Chem.*, 2006, (21), 4924–4933.
29 K. Hiraki, Y. Fuchita and K. Takechi, *Inorg. Chem.*, 1981, **20**, 4316–4320.
30 K. Hiraki and Y. Fuchita, *Inorg. Synth.*, 1989, **26**, 208–211.
31 T. A. Stephenson, S. M. Morehouse, A. R. Powell, J. P. Heffer and G. Wilkinson, *J. Chem. Soc.*, 1965, 3632–3640.
32 M. Pfeffer, E. Wehman and G. van Koten, *J. Organomet. Chem.*, 1985, **282**, 127–131.
33 K. Hiraki, Y. Fuchita, H. Nakaya and S. Takakura, *Bull. Chem. Soc. Jpn.*, 1979, **52**, 2531–2534.
34 R. G. Pearson, *Inorg. Chem.*, 1973, **12**, 712–713.
35 V. A. Polyakov and A. D. Ryabov, *J. Chem. Soc., Dalton Trans.*, 1986, 589–593.
36 M. L. Zanini, M. R. Meneghetti, G. Ebeling, P. R. Livotto, F. Rominger and J. Dupont, *Inorg. Chim. Acta*, 2003, **350**, 527–536.
37 G.-D. Roiban, E. Serrano, T. Soler, M. Contel, I. Grosu, C. Cativiela and E. P. Urriolabeitia, *Organometallics*, 2010, **29**, 1428–1435.
38 A. G. Orpen, L. Brammer, F. H. Allen, O. Kennard, D. G. Watson and R. Taylor, *J. Chem. Soc., Dalton Trans.*, 1989, S1–S83.
39 V. K. Kravtsov, Y. M. Chumakov, S. A. D'yachenko, V. N. Biyushkin, M. I. Bureneva and T. I. Malinovskii, *J. Struct. Chem.*, 1990, **31**, 311–317.
40 J. Vicente, I. Saura-Llamas, J. Cuadrado and M. C. Ramírez de Arellano, *Organometallics*, 2003, **22**, 5513–5517.
41 M. La Deda, M. Ghedini, I. Aiello, T. Pugliese, F. Barigelletti and G. Accorsi, *J. Organomet. Chem.*, 2005, **690**, 857–861.
42 M. Ghedini, D. Pucci, G. Calogero and F. Barigelletti, *Chem. Phys. Lett.*, 1997, **267**, 341–344.
43 M. D. Santana, R. García-Bueno, G. García, G. Sánchez, J. García, J. Pérez, L. García and J. L. Serrano, *Dalton Trans.*, 2011, **40**, 3537–3546.
44 A. J. Lees, *Chem. Rev.*, 1987, **87**, 711–743.
45 C. A. Craig and R. J. Watts, *Inorg. Chem.*, 1989, **28**, 309–313.
46 I. E. Pomestchenko and F. N. Castellano, *J. Phys. Chem. A*, 2004, **108**, 3485–3492.
47 J. E. McGarrah and R. Eisenberg, *Inorg. Chem.*, 2003, **42**, 4355–4365.
48 J. E. Bercaw, A. C. Durrell, H. B. Gray, J. C. Green, N. Hazari, J. A. Labinger and J. R. Winkler, *Inorg. Chem.*, 2010, **49**, 1801–1810.
49 A. Diez, J. Forniés, S. Fuertes, E. Lalinde, C. Larraz, J. A. López, A. Martín, M. T. Moreno and V. Sicilia, *Organometallics*, 2009, **28**, 1705–1718.
50 M. Juribašić, M. Ćurić, K. Molčanov, D. Matković-Čalogović and D. Babić, *Dalton Trans.*, 2010, **39**, 8769–8778.
51 S. W. Lai, T. C. Cheung, M. C. W. Chan, K. K. Cheung, S. M. Peng and C. M. Che, *Inorg. Chem.*, 2000, **39**, 255–262.
52 K. A. Van Houten, D. C. Heath, C. A. Barringer, A. L. Rheingold and R. S. Pilato, *Inorg. Chem.*, 1998, **37**, 4647–4653.
53 F. Neve, A. Crispini and S. Campagna, *Inorg. Chem.*, 1997, **36**, 6150–6156.
54 Q. Wu, A. Hook and S. Wang, *Angew. Chem., Int. Ed.*, 2000, **39**, 3933–3935.
55 S.-C. Chan, M. C. W. Chan, Y. Wang, C.-M. Che, K.-K. Cheung and N. Zhu, *Chem.–Eur. J.*, 2001, **7**, 4180–4190.
56 J. E. McGarrah and R. Eisenberg, *Inorg. Chem.*, 2003, **42**, 4355–4365.
57 D. M. Manuta and A. J. Lees, *Inorg. Chem.*, 1986, **25**, 3212–3218.
58 W. Kaim, S. Kohlmann, S. Ernst, B. Olbrich-Deussner, C. Bessenbacher and A. Schulz, *J. Organomet. Chem.*, 1987, **321**, 215–226.

59 W. Kaim and S. Kohlmann, *Inorg. Chem.*, 1986, **25**, 3306–3310.
60 T. R. Miller and I. G. Dance, *J. Am. Chem. Soc.*, 1973, **95**, 6970–6979.
61 E. S. Dodsworth and A. B. P. Lever, *Inorg. Chem.*, 1990, **29**, 499–503.
62 A. B. P. Lever, *Inorganic Electronic Spectroscopy*, Elsevier, Amsterdam, 1984, p208.
63 E. S. Dodsworth, A. B. P. Lever and Chem, *Phys. Lett.*, 1984, **112**, 567–570.
64 H. Saito, J. Fujita and K. Saito, *Bull. Chem. Soc. Jpn.*, 1968, **41**, 863–874.
65 V. M. Miskowski and V. H. Houlding, *Inorg. Chem.*, 1989, **28**, 1529–1533.
66 F. Neve, A. Crispini, C. Di Pietro and S. Campagna, *Organometallics*, 2002, **21**, 3511–3518.
67 M. Klessinger and J. Michl, *Excited States and Photochemistry of Organic Molecules*, VCH, New York, 1995.
68 F. Neve, A. Crispini, F. Loiseau and S. Campagna, *J. Chem. Soc., Dalton Trans.*, 2000, 1399–1401.
69 M. Ghedini, I. Aiello, M. La Deda and A. Grisolia, *Chem. Commun.*, 2003, 2198–2199.
70 G. R. Crosby, *Acc. Chem. Res.*, 1975, **8**, 231–238.
71 G. R. Rosa, G. Ebeling, J. Dupont and A. L. Monteiro, *Synthesis*, 2003, 2894–2897.
72 R. F. Kubin and A. N. Fletcher, *J. Lumin.*, 1983, **27**, 455–462.
73 J. N. Demas and G. A. Crosby, *J. Phys. Chem.*, 1971, **75**, 991–1024.
74 S. Fery-Forgues and D. J. Lavabre, *J. Chem. Educ.*, 1999, **76**, 1260–1264.
75 *Kappa CCD Operation Manual*, ed. B. V. Nonius, Delft, The Netherlands, 1997.
76 G. M. Sheldrick, "SHELXS-97 Program for Crystal Structure Determination", *Acta Crystallogr., Sect. A: Found. Crystallogr.*, 1990, **46**, 467–473.
77 G. M. Sheldrick, *SHELXL-97, Program for refinement of crystal structures*, University of Göttingen, Germany, 1997.
78 A. L. Spek, *J. Appl. Crystallogr.*, 2003, **36**, 7–13.

